J. Fluid Mech. (1996), vol. 319, pp. 151–170

On a class of unsteady boundary layers of finite extent

By W.R.C. PHILLIPS†

Department of Mechanical and Aeronautical Engineering,
Clarkson University, Potsdam, NY 13699-5725, USA

(Received 20 October 1995 and in revised form 2 February 1996)

A class of unsteady boundary layers that form on flat extensible surfaces of finite but increasing length in otherwise stagnant surroundings is considered. The surface length $\bar{R}$ is assumed to grow with time as t^p where $p > 0$ and the velocity at any location $0 \leqslant \bar{r} \leqslant \bar{R}$ on the surface as $t^{p-np-1}\bar{r}^n$, where $n \geqslant 0$. The problem is cast into similarity variables and the governing parabolic differential equation shown to exhibit, for various combinations of n and p, regions of mixed mathematical diffusivity and reversals in the direction of convection of vorticity. Equations depicting such behaviour are usually termed singular parabolic and are here classified as follows: type-0, in which the mathematical diffusivity may be either positive or mixed but in which there are no reversals in the direction of convection of vorticity; type-1, in which the mathematical diffusivity may be either positive or mixed but in which there are reversals in the direction of convection of vorticity. Both types are shown to occur. Moreover while type-0 flows occur only when $n = 1$ and form with an unsteady separated stagnation point at the origin, type-1 flows occur only for $0 \leqslant n < 1$ and form with a steady stagnation point at the origin. Type-1 flows are further characterized by boundary layers with zero displacement thickness both at the origin and leading edge. Because singular parabolic equations require two initial conditions plus boundary conditions to ensure uniqueness, they are here treated numerically in a manner akin to elliptic boundary value problems. A successive-approximation implicit scheme was thus used and a wide range of cases solved in the parameter range $n \in [0, 1]$, $p \in (0, 2]$. Amongst other things, it is shown that type-0 flows have lower drag than their type-1 counterparts. It is further shown that the drag on a flat rigid surface of finite length moving in its own plane at constant velocity and being continuously produced at the origin is higher than on a corresponding length of either a semi-infinite surface likewise produced or a semi-infinite plate in an aligned uniform stream; however if the surface is extensible and $n > \frac{1}{2}$ the converse is true.

1. Introduction

We consider a class of unsteady boundary layers that form on flat impermeable surfaces of finite but increasing length, in otherwise quiescent fluid. Such boundary layers have relevance to those which form in open bodies of deep water due to gusting winds (Taylor 1959) or growing oil slicks (Fay 1969). Accordingly they occur on plates or membranes of finite length emerging into otherwise stagnant fluid from

† Present address: Department of Theoretical and Applied Mechanics, University of Illinois at Urbana-Champaign, Urbana, IL 61801-2935, USA.

a slit in a wall; they also form behind a moving shock wave on a flat plate (Lam & Crocco 1959). Characteristic of some of the boundary layers so formed is that they have beginnings (i.e. zero displacement thickness) at both the leading edge and origin of the surface: the flow being asymptotic to a Blasius (1908) boundary layer at the former and on occasion a variant of a Sakiadis (1961) boundary layer at the latter (see §§4, 5). It is this class of boundary layers that are of interest here.

Not surprisingly the parabolic differential equation governing such motion has peculiar properties and cannot be treated numerically in a manner akin to 'well posed' parabolic equations. That is, the sign of the diffusive term, to which we here refer as the diffusivity or more precisely the mathematical diffusivity, is positive throughout the domain in well-posed parabolic differential equations, which are uniquely determined by given boundary conditions and an initial condition. Ill-posed parabolic equations on the other hand have negative diffusivity. But the boundary layers of interest are described by an equation that admits an essential singularity or stagnation point downstream of the leading edge in concert with diffusivity of mixed sign, so uniqueness is assured only when, in addition to appropriate boundary conditions, initial conditions are specified at each end of the boundary layer (Stewartson 1951; Brown & Stewartson 1969). Lam & Crocco (1959) term such equations, 'singular parabolic'.

Obtaining numerical solutions in the region where the diffusivity is mixed is not straightforward: indeed many years passed before Hall (1969) and Dennis (1972) solved Stewartson's (1951) problem of a semi-infinite flat plate set impulsively into motion in its own plane. To proceed, Hall deferred to primitive rather than similarity variables while Dennis retained similarity variables but divided the solution domain into zones based on the characteristics of the mathematical diffusivity; methods of solution were then adjusted from zone to zone and artificial damping was required in order to stabilize the calculation. Similar approaches using Crocco variables were employed by Ban & Kuerti (1969) and Walker & Dennis (1972) to treat the singular parabolic equation describing the unsteady boundary layer flow in a shock tube, although Wang (1983, 1985) later found that the problems of both Stewartson and Lam & Crocco could be handled in a manner akin to elliptic differential equations, provided the two initial conditions are specified consistently.

Boundary layers on flat stretching surfaces in otherwise stagnant unbounded fluid have attracted considerable attention (Stuart 1966; Crane 1970; Wang 1984; Banks & Zaturska 1986, and references therein), but apparently only those due to Buckmaster (1973), Foda & Cox (1980) and Jensen (1995) deal with boundary layers beneath extensible surfaces of finite extent, and of these studies (see §3) only Foda & Cox deal with boundary layers that have beginnings both at the origin and leading edge of the surface.

Our object in the present work therefore is to consider a broad range of unsteady boundary layers of finite but increasing length that admit multiple beginnings. We thus consider a surface of length $\bar{R}$ that increases with time t as t^p, where $p > 0$ and on which the velocity at any point $0 \leqslant \bar{r} \leqslant \bar{R}$ grows as $t^{p-np-1}\bar{r}^n$, where $n \geqslant 0$. The index p is continuously variable, although physically realizable scenarios in nature, at least with spreading oil, decree that p be rational. In §2 we cast the problem into similarity variables; then in §3 show that the governing differential equation exhibits, for various combinations of n and p, regions of mixed mathematical diffusivity and reversals in the direction of convection of vorticity. The resulting singular parabolic behaviour is thus classified as follows: type-0, in which the diffusivity may be either positive or mixed but in which there are no reversals in the direction of convection of vorticity; and type-1, in which the diffusivity may be either positive or mixed, but

in which there are reversals in the direction of convection of vorticity. It is further shown that both types 0 and 1 occur in the range $0 \leqslant n \leqslant 1$ with $p > 0$.

Type-0 flows are found to occur only when $n = 1$ and form, as previously noted by Jensen (1995), with what Ma & Hui (1990) term an 'unsteady separated stagnation point' (see §4) at the origin. Such stagnation points admit a plethora of solutions, but Buckmaster (1973) argues that the only relevant solutions are those which depict exponential decay (with distance from the surface). We show that two exponentially decaying solutions exist at each p. Those solutions specified by the upper branch (of such solutions) admit forward-only flow and include particular cases of Buckmaster and Jensen, while solutions specified by the lower branch admit flow reversals, unless $p < 6.8 \times 10^{-4}$, in which case the solutions are identical to their upper-branch counterparts but of opposite sign.

Type-1 flows on the other hand form with a 'steady stagnation point' (see Ma & Hui) at the origin, occur only for $0 \leqslant n < 1$ and admit forward-only flow. Such flows are further characterized by boundary layers with zero displacement thickness both at the origin and leading edge.

In §5 we look briefly at the leading-edge flow and show it to be asymptotic to that of a Blasius (1908) boundary layer for all n and p, a result which concurs with previous findings at specific values of p (Buckmaster; Foda & Cox; Jensen). Our numerics are outlined in §6. A wide range of cases in the parameter range $n \in [0,1]$, $p \in (0,2]$ were solved numerically and our results are given and discussed in §7. The results show, *inter alia*, that type-0 flows have lower drag than their type-1 counterparts. The results also show that the drag on a flat rigid surface of finite length moving in its own plane at constant velocity and being continuously produced at the origin is higher than that on corresponding lengths of either a semi-infinite surface likewise produced (i.e. a Sakiadis boundary layer) or a semi-infinite plate in an aligned uniform stream (i.e. a Blasius boundary layer), but that if the surface is extensible and $n > \frac{1}{2}$, the converse is true.

2. The boundary layer

Consider a flat impermeable surface of length $\bar{R}$ which originates at the origin (which is fixed in space) and evolves in the absence of pressure gradients in the positive $\bar{r}$-direction into otherwise quiescent unbounded fluid. Owing to the non-slip condition, the surface drags fluid with it, giving rise to a boundary layer flow in $0 \leqslant \bar{r} \leqslant \bar{R}$, $0 \leqslant \bar{z} < \infty$ with velocity components $\bar{v}_{\bar{r}}(\bar{r},\bar{z},t)$ and $\bar{v}_{\bar{z}}(\bar{r},\bar{z},t)$ in the $\bar{r}$-, and $\bar{z}$-directions. Provided $\bar{R} \gg \bar{\delta}$, where $\bar{\delta}$ is the characteristic thickness of the boundary layer, we may invoke the long-wave assumption and ignore $\partial^2 \bar{v}_{\bar{r}}/\partial \bar{r}^2$. The flow field, be it planar or axisymmetric, is then described by the unsteady momentum equation

$$\frac{\partial \bar{v}_{\bar{r}}}{\partial t} + \bar{v}_{\bar{r}} \frac{\partial \bar{v}_{\bar{r}}}{\partial \bar{r}} + \tilde{v}_{\bar{z}} \frac{\partial \bar{v}_{\bar{r}}}{\partial \bar{z}} = \frac{\partial^2 \bar{v}_{\bar{r}}}{\partial \tilde{z}^2} \tag{2.1}$$

in combination with the planar or axisymmetric continuity equations,

$$\frac{\partial \bar{v}_{\bar{r}}}{\partial \bar{r}} + \frac{\partial \tilde{v}_{\bar{z}}}{\partial \tilde{z}} = 0 \quad \text{or} \quad \frac{1}{\bar{r}} \frac{\partial (\bar{r} \bar{v}_{\bar{r}})}{\partial \bar{r}} + \frac{\partial \tilde{v}_{\bar{z}}}{\partial \tilde{z}} = 0, \tag{2.2}$$

in which we have used kinematic viscosity ν to rescale $\bar{v}_{\bar{z}}$ and $\bar{z}$ as $\tilde{v}_{\bar{z}} = \bar{v}_{\bar{z}}/\nu^{1/2}$, $\tilde{z} = \bar{z}/\nu^{1/2}$. Appropriate boundary conditions are

$$\bar{v}_{\bar{z}} = 0 \ \text{ on } \ \bar{z} = 0 \quad \text{and} \quad \bar{v}_{\bar{r}} \to 0 \ \text{ as } \ \bar{z} \to \infty.$$

The surface is assumed to grow as t^p, and so we seek a similarity solution by rescaling our dependent variables as

$$v_r(r,z) = \mathscr{M} t^{1-p} \bar{v}_{\bar{r}} \quad \text{and} \quad v_z(r,z) = \nu^{-1/2} t^{1/2} \bar{v}_{\bar{z}}, \tag{2.3a}$$

and our independent variables as

$$r = \mathscr{M} t^{-p} \bar{r} \quad \text{and} \quad z = \nu^{-1/2} t^{-1/2} \bar{z}. \tag{2.3b}$$

Here $\mathscr{M}$ is a constant whose details depend upon the physical problem at hand. These variables transform (2.1) into

$$(p-1)v_r - pr\frac{\partial v_r}{\partial r} - \frac{1}{2}z\frac{\partial v_r}{\partial z} + v_r\frac{\partial v_r}{\partial r} + v_z\frac{\partial v_r}{\partial z} = \frac{\partial^2 v_r}{\partial z^2} \tag{2.4}$$

and (2.2) into

$$\frac{\partial v_r}{\partial r} + \frac{\partial v_z}{\partial z} = 0 \quad \text{or} \quad \frac{1}{r}\frac{\partial (r v_r)}{\partial r} + \frac{\partial v_z}{\partial z} = 0. \tag{2.5}$$

Having reduced the number of independent variables by one, we now reduce the number of dependent variables by one by introducing a dimensionless stream function ψ that satisfies the planar form of (2.5) and is defined by

$$v_r = \frac{\partial \psi}{\partial z}, \quad v_z = -\frac{\partial \psi}{\partial r}.$$

Equation (2.4) may then be written, with subscripts on ψ denoting differentiation,

$$(p-1)\psi_z - pr\psi_{rz} - \tfrac{1}{2}z\psi_{zz} + \psi_z\psi_{rz} - \psi_r\psi_{zz} = \psi_{zzz}. \tag{2.6}$$

Accordingly, the axisymmetric counterpart to (2.6) is obtained by writing

$$v_r = \frac{1}{r}\frac{\partial \psi}{\partial z}, \quad v_z = -\frac{1}{r}\frac{\partial \psi}{\partial r}$$

to yield

$$(p-1)\psi_z - pr(\psi_{rz} - \frac{1}{r}\psi_z) - \tfrac{1}{2}z\psi_{zz} + \frac{1}{r}\psi_z(\psi_{rz} - \frac{1}{r}\psi_z) - \frac{1}{r}\psi_r\psi_{zz} = \psi_{zzz}. \tag{2.7}$$

Finally we allow the velocity on $z = 0$, v_r^* say, to vary as r^n, where $n \geqslant 0$ is a constant. Then because $\bar{R} = \mathscr{M}^{-1} t^p R$ at the leading edge, we see that $v_r^* = pR$ there, and thus that

$$v_r^* = pR^{1-n} r^n \tag{2.8}$$

for any $0 \leqslant r \leqslant R$.

3. Parabolic or singular parabolic behaviour?

The hallmark of parabolic equations that describe unsteady boundary layers of finite length is the presence of an essential singularity or stagnation point aft of the leading edge. In our case this occurs in (2.4) at $r = 0$. We shall employ two indicators to determine the presence of this irregularity: diffusivity of mixed sign and a reversal in the direction of convection of vorticity; the two are not equivalent.

To isolate the first we assume positive diffusivity in at least part of the domain $r \in [0, R]$ and $z \in [0, \infty]$, and seek regions where the diffusivity is negative; this we do by viewing (2.4) on $z = 0$ where it reduces to

$$\frac{\partial^2 v_r^*}{\partial z^2} = pR^{1-n} r^n \{p - np - 1 + np(r/R)^{n-1}\}.$$

Observe that $\partial^2 v_r^*/\partial z^2$ is negative for $0 < p < 1$ when $n = 0$ or 1 and for some $r \in [0, R]$ for other $n \in (0, 1)$. The diffusivity is also negative for some $r \in [0, R]$ when $n > 1$ for all $p > 0$, but vanishes at $n = 1$, $p = 1$, and is strictly positive for $n \in [0, 1]$ when $p > 1$. Thus we expect diffusivity of mixed sign for all $n \geqslant 0$ and $p > 0$ except $n \in [0, 1]$ when $p \geqslant 1$.

Consider now the direction of convection of vorticity and restrict attention to the boundaries of the flow domain; furthermore assume $v_r \geqslant 0$ throughout the domain and note that, in accord with the long-wave assumption, the dominant component of vorticity is $\omega = \partial v_r/\partial z$. Then on differentiating (2.4) with respect to z we find

$$(2p-1)\omega + \frac{\partial}{\partial r}[(v_r - pr)\omega] + \frac{\partial}{\partial z}[(v_z - \tfrac{1}{2}z)\omega] = \frac{\partial^2 \omega}{\partial z^2}, \tag{3.1}$$

which indicates that vorticity is convected in the flow field $(v_r - pr, v_z - \frac{1}{2}z)$.

Consider first the flow along the $z = 0$ axis. Here $v_r^* - pr = pr^n(R^{1-n} - r^{1-n})$ and we see that

$$v_r^* - pr \quad \left\{ \begin{array}{ll} < 0 & \text{for } n > 1 \\ = 0 & \text{for } n = 1 \\ > 0 & \text{for } n < 1 \end{array} \right\} \quad \text{on} \quad z = 0 \quad \text{for} \quad 0 \leqslant r < R \tag{3.2}$$

while $v_z - \frac{1}{2}z = 0$ for $0 \leqslant r < R$. Next, as $z \to \infty$ we see that $v_r - pr < 0$ and $v_z - \frac{1}{2}z < 0$ for all $0 < r \leqslant R$.

Accordingly, if in view of (2.8) we write (as $r \to 0$ or R) that $v_r = pR^{1-n}r^n \mathscr{F}_r'(zr^{-\beta})$ where $\beta = (1-n)/2$ for $n \leqslant 1$ and 0 for $n \geqslant 1$ (see §4), then as $r \to 0$, we have $v_r/pr = (r/R)^{n-1}\mathscr{F}_0'(zr^{-\beta})$ and $\operatorname{sgn}(v_r - pr)$ depends on $\lim_{r\to 0}(r/R)^{n-1}\mathscr{F}_0'(zr^{-\beta})$. Then because $\mathscr{F}_r'(0) = 1$ and if we require $\mathscr{F}_r' \to 0$ exponentially fast as $zr^{-\beta} \to \infty$ (see §4), it follows that

$$v_r - pr \quad \left\{ \begin{array}{ll} < 0 & \text{for } n > 1 \\ = 0 & \text{for } n = 1 \\ < 0 & \text{for } n < 1 \end{array} \right\} \quad \text{on} \quad r = 0 \quad \text{for} \quad 0 < z < \infty. \tag{3.3}$$

Furthermore $v_z - \frac{1}{2}z \leqslant 0$ for all n and $0 \leqslant z < \infty$ at both $r = 0$ and R. Lastly, at $r = R$ we have $v_r - pr = Rp(\mathscr{F}_R' - 1) \leqslant 0$ for $0 \leqslant z < \infty$.

Observe that p, which by definition is positive, plays no role in determining the direction of convection of vorticity; the key parameter is n. Specifically, with $n \geqslant 1$, there is no convection of vorticity in the positive r-direction and (2.4) may thus be solved numerically in one sweep in the negative r-direction (for $r \in [0, R]$) beginning at $r = R$. That is, although the diffusivity is mixed for $0 < p < 1$ when $n \geqslant 1$, the boundary layer begins only at $r = R$ and (2.4) is, for computational purposes, parabolic. However because a stagnation point is present at $r = 0$ in (2.4) in such circumstances, and because we cannot march through $r = 0$, we shall here refer to (2.4) as singular parabolic type-0. Furthermore, because type-0 can occur both with $(0 < p < 1)$ and without $(p \geqslant 1)$ mixed diffusivity, we use the respective notations SP0m and SP0. The works of Buckmaster (1973; $n = 1$, $p = \frac{3}{8}$) and Jensen (1995; $n = 1$, $p = \frac{1}{2}, \frac{3}{8}$) thus belong to the class SP0m. For $n < 1$, however, vorticity is convected in both the positive *and* negative r-directions; moreover the diffusivity is mixed, at least in the parameter range $0 < p < 1$ for $0 \leqslant n < 1$. In this instance standard numerical marching techniques will fail for all r and so we describe (2.4) as singular parabolic type-1m (SP1m). Foda & Cox's (1980; $p = \frac{3}{4}$) study of surface-tension-driven oil-spreading on water belongs to this class, although their v_r^*

is somewhat more complicated than those described by r^n. Reversals in the direction of convection of vorticity continue for $p \geqslant 1$, a range in which the diffusivity is not mixed but in which marching techniques again fail; so here (2.4) (for $0 \leqslant n < 1$) is SP1.

Finally, although our intent is to concentrate on cases for which $0 \leqslant n < 1$ for all $p > 0$, it behoves us to also explore the case $n = 1$. We begin by defining initial value problems at the origin and leading edges of our extensible surface.

4. The boundary layer in the region $r \to 0$

Consider the boundary layer in the vicinity of $r = 0$. Here, in view of (2.8), we seek a solution of the form $v_r = r^n f(\eta)$, where $\eta = zr^{-\beta}$ and β is to be determined; our planar and axisymmetric stream functions are thus

$$\psi = r^{n+\beta}\chi(\eta) \quad \text{and} \quad \psi = r^{n+\beta+1}\chi(\eta). \tag{4.1}$$

Then, substitution of (4.1) into (2.6) or (2.7) admits, in the limit $r \to 0$, two possibilities for β. The first, $\beta = (1-n)/2$, yields

$$\chi''' - n(\chi')^2 + \alpha\chi\chi'' = (p - pn - 1)r^{1-n}(\chi' + \tfrac{1}{2}\eta\chi'') \tag{4.2}$$

where $\alpha = (n+1)/2$ or $\alpha = (n+3)/2$ with the boundary conditions

$$\chi = 0, \quad \chi' = f(0) = pR^{1-n} \quad \text{on} \quad \eta = 0 \quad \text{and} \quad \chi' = 0 \quad \text{as} \quad \eta \to \infty. \tag{4.3}$$

Note that the right-hand side of (4.2) must be retained as $n \to 1$. We see why by viewing the displacement thickness $\delta^* = \int_0^\infty (v_r/v_r^*)\mathrm{d}z = r^{(1-n)/2}\chi(\infty)/pR^{1-n}$. Observe that $\delta^* \to 0$ as $r \to 0$ for $n < 1$, is non-zero but finite when $n = 1$ and is singular for $n > 1$, each reflecting a change in both the structure of the boundary layer and the differential equation that describes it. We also see that (4.2) reduces, for $n > 1$, to $\chi' + \frac{1}{2}\eta\chi'' = 0$ which does not admit solutions in accord with (4.3). In consequence $\beta = (1-n)/2$ and (4.2) are appropriate only when $n \leqslant 1$.

The second possibility is restricted to $n \geqslant 1$; here $\beta = 0$ and

$$\chi''' + \tfrac{1}{2}\eta\chi'' - (p - pn - 1)\chi' = r^{1-n}[n(\chi')^2 - \gamma\chi\chi''] \tag{4.4}$$

where $\gamma = n$ or $n+1$ with (4.3). Again the right-hand side must be retained as $n \to 1$, at which point (4.2) and (4.4) are equivalent. But as we saw in §3 the range of n of most interest in the present work is $0 \leqslant n \leqslant 1$, so for that reason we shall not discuss (4.4) further.

Looking first then to the case $n = 1$, we have

$$\chi''' - (\chi')^2 + \alpha\chi\chi'' = -\chi' - \tfrac{1}{2}\eta\chi'' \tag{4.5}$$

with the boundary conditions

$$\chi = 0, \quad \chi' = p \quad \text{on} \quad \eta = 0; \quad \chi' = 0 \quad \text{as} \quad \eta \to \infty. \tag{4.6}$$

Buckmaster (1973) studied (4.5) and showed that (4.6) do not ensure uniqueness: rather (4.6) are satisfied by any $\chi''(0)$ and admit solutions that decay either algebraically or exponentially with large η. But with the exception of isolated points, exponential decay is required in laminar boundary layers (Brown & Stewartson 1965), so he chose to impose such decay, which is tantamount to a uniqueness assumption. He identified $\chi''(0) = -0.0124$ as the only value of skin friction (at $p = \frac{3}{8}$) for which the decay at the boundary layer edge is exponential and for which there is no reversed flow.

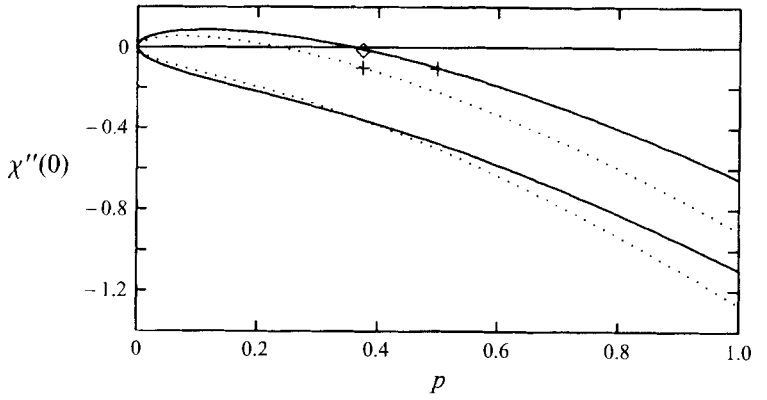

FIGURE 1. The variation of $\chi''(0)$ with p for exponentially decaying unsteady separated stagnation point flow ($n = 1$) at the origin. Continuous line, planar flow; dotted line, radial flow. ◇, Buckmaster (1973); +, Jensen (1995).

In fact for each p there are two values of $\chi''(0)$ that lead to exponential decay, as we see by considering the limit $p \to 0$. Here we find numerically that

$$\lim_{p\to 0} \chi''(0) = 0\pm,$$

the 0+ and 0− values invoking identical solutions that are reversed in sign, thereby requiring $\chi''' + \chi' + \frac{1}{2}\eta\chi'' = 0$ and $(\chi')^2 - \alpha\chi\chi'' = 0$ as $p \to 0$. Moreover the flow is strictly unidirectional, being forward when $\chi''(0) = 0+$. But this symmetry is soon broken as p increases, leading to an upper and lower branch for $\chi''(0)$, as shown in figure 1.

Observe that $\chi''(0) > 0$ for some p on the upper branch, indicating that the velocity in the boundary layer exceeds that at the surface (see also §7.3). But while the flow remains strictly forward for all $p > 0$ (see figure 2*a*) on this branch, that is not the case on the lower branch, which (for $p > 6.8 \times 10^{-4}$) gives rise to both forward and reversed flow (figure 2*b*). Thus to ensure uniqueness, we must impose not only exponentially fast decay but also specify whether the flow may or may not reverse.

Two solutions – one that depicts forward-only flow, the other in which the flow reverses – were also observed by Ma & Hui (1990) in a general study of what they term 'unsteady separated stagnation point flows', a class into which (4.5) falls. Conversely, the absence of the right-hand side of (4.5) leads to 'steady stagnation point flow' which does have a unique solution.

Turning then to $n < 1$, we see that the right-hand or 'unsteady' component of (4.2) vanishes as $r \to 0$, so that we may assume (4.2) has a unique solution for each $f(0)$. We thus consider the differential equation

$$\lambda''' - n(\lambda')^2 + \alpha\lambda\lambda'' = 0 \tag{4.7}$$

for $\lambda(\eta)$ with the boundary conditions

$$\lambda = 0, \quad \lambda' = 1 \quad \text{on} \quad \eta = 0; \quad \lambda' \to 0 \quad \text{as} \quad \eta \to \infty, \tag{4.8}$$

such that

$$\chi(\eta) = (pR^{1-n})^{1/2}\lambda\{(pR^{1-n})^{1/2}\eta\}. \tag{4.9}$$

Then with $n = 0$, equation (4.7) reduces to $\lambda''' + \alpha\lambda\lambda'' = 0$. This equation describes the laminar boundary layer flow on a flat rigid surface moving in its own plane in the

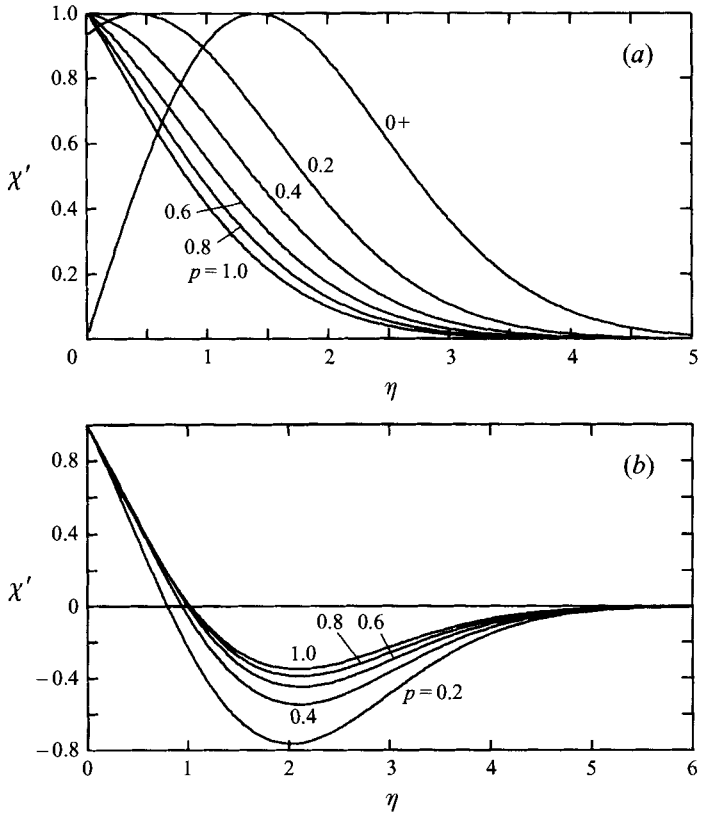

FIGURE 2. Velocity distributions (normalized by their peak value) arising from (*a*) upper-branch and (*b*) lower-branch values of the planar $\chi''(0)$ curve.

r-direction, the surface being continuously produced at $r = 0$, where $r = 0$ is fixed in space. Sakiadis (1961) solved the planar ($\alpha = \frac{1}{2}$) case and it, and the solution to its axisymmetric counterpart ($\alpha = \frac{3}{2}$), are sketched in figure 3.

Lastly, for $0 \leqslant n < 1$, equation (4.7) has an approximate solution of the form (Foda & Cox 1980)

$$\lambda(\eta) = \mathscr{A}(1 - \mathscr{B}e^{-\alpha\mathscr{A}\eta} + \mathscr{C}e^{-2\alpha\mathscr{A}\eta} + \mathscr{D}e^{-3\alpha\mathscr{A}\eta} + \mathscr{E}e^{-4\alpha\mathscr{A}\eta} + \ldots) \tag{4.10}$$

where $\mathscr{A}, \mathscr{B}, \mathscr{C}, \mathscr{D}$ and $\mathscr{E}$ are constants that follow from (4.8). Foda & Cox treat the planar case $\alpha = (n+1)/2$, but it is evident that (4.10) is also a solution to (4.7) for the case $\alpha = (n+3)/2$ and we find in general that

$$\mathscr{C} = \frac{(5\alpha - n)^2(\alpha - n)}{64\alpha^3}, \quad \mathscr{D} = -\frac{(5\alpha - 4n)(5\alpha - n)(\alpha - n)}{288\alpha^3}, \quad \mathscr{E} = \frac{(\alpha - n)^3}{192\alpha^3}.$$

Further, from the boundary condition $\lambda(0) = 0$, we see that $\mathscr{B} = 1 + \mathscr{C} + \mathscr{D} + \mathscr{E}$, while from $\lambda'(0) = 0$ we obtain $\mathscr{A} = [\alpha(\mathscr{B} - 2\mathscr{C} - 3\mathscr{D} - 4\mathscr{E})]^{-1/2}$.

To conclude therefore, we see that the irregularity at the origin, in what we refer to as SP0 flows (for $n = 1$, see §3), presents itself as an unsteady separated stagnation point, while that in SP1 flows, at least of the type under consideration here, presents itself, for $0 \leqslant n < 1$, as a steady stagnation point.

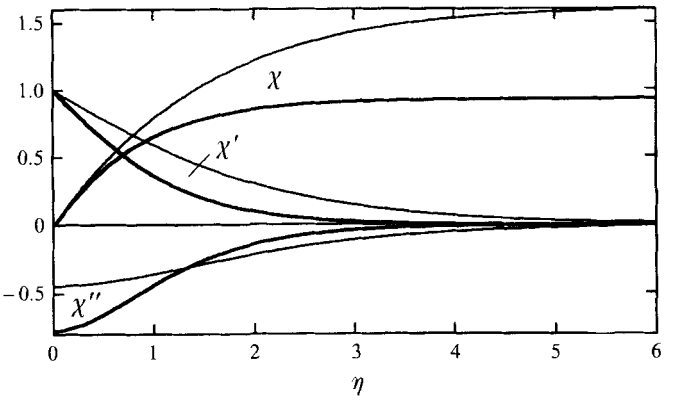

FIGURE 3. Steady stagnation point flow ($n = 0$) at the origin showing the function χ and its derivatives. Thin curve, planar flow (Sakiadis 1961); thick curve, radial flow.

5. The boundary layer near the leading edge, $r \to R$

To isolate the dominant terms in (2.6), (2.7) in the region of the leading edge $r \to R$, we relocate the origin at the leading edge and introduce the variable s, as $r = R - s$. Then since the boundary layer must grow as $s^{1/2}$, (2.6) and (2.7) respectively become, as $s \to 0$,

$$pR\psi_{sz} - \psi_z\psi_{sz} + \psi_s\psi_{zz} = \psi_{zzz}, \tag{5.1}$$

$$pR\left(\psi_{sz} + \frac{1}{R}\psi_z\right) - \frac{1}{R}\psi_z\left(\psi_{sz} + \frac{1}{R}\psi_z\right) + \frac{1}{R}\psi_s\psi_{zz} = \psi_{zzz}. \tag{5.2}$$

Then on writing $\zeta = zs^{-1/2}$ with

$$\psi = s^{1/2}\kappa(\zeta), \tag{5.3}$$

the planar (5.1) and axisymmetric (5.2) equations become

$$\kappa''' - \tfrac{1}{2}\kappa\kappa'' + \tfrac{1}{2}pR\zeta\kappa'' = 0 \quad \text{and} \quad \kappa''' - \frac{1}{2R}\kappa\kappa'' + \tfrac{1}{2}pR\zeta\kappa'' = 0, \tag{5.4}$$

with the boundary conditions

$$\kappa = 0 \text{ and } \kappa' = pR \quad \text{or} \quad \kappa' = pR^2 \text{ on } \zeta = 0 \text{ and } \kappa' \to 0 \text{ as } \zeta \to \infty.$$

Lastly, on setting $\kappa(\zeta) = pR\zeta + \phi(\zeta)$ or $\kappa(\zeta) = pR^2\zeta + R\phi(\zeta)$, where $\phi(\zeta) = -(pR)^{1/2}g[(pR)^{1/2}\zeta]$, we recover the Blasius (1908) equation $g''' + \frac{1}{2}gg'' = 0$ with $g = 0$, $g' = 0$ on $\zeta = 0$ and $g' \sim 1$ as $\zeta \to \infty$. So, further to Buckmaster's (1973), Foda & Cox's (1980) and Jensen's (1995) observations for specific values of p, we see that (from the reference frame of the leading edge of the surface) the flow field is asymptotic to that of a Blasius boundary layer for all p and n, whether the surface is planar or axisymmetric.

Finally, the stream function becomes

$$\psi = s^{1/2}\{pR\zeta + \phi(\zeta)\} \quad \text{or} \quad \psi = s^{1/2}R\{pR\zeta + \phi(\zeta)\} \text{ as } s \to 0, \tag{5.5}$$

while the displacement thickness $\delta^* = s^{1/2}/pR\kappa(\infty)$.

6. Numerics

In view of the singular nature of the solution at $r = 0$ and R, it is prudent, prior to any numerical treatment of (2.4), to map it to a form that directly recovers (4.2) when $r = 0$ and (5.4) at $r = R$. This is achieved as follows: first since $\psi(r, z)$ takes the form $r(r^m)^{((n+1)/2m)-1}\mathcal{G}(r^m, z)$ near the origin, and because v_r is odd, we set $m = 2$. Then, in order to work in the domain $x \in [0, 1]$, $y \in [0, \infty]$ and in view of the form of the independent variables η and ζ, we let

$$x = (r/R)^2 \quad \text{and} \quad y = \frac{z}{(1-x)^{1/2}x^{(1-n)/4}}. \tag{6.1}$$

Finally, because ψ has the form (4.1) near the origin and (5.3) near the leading edge, we write (for the planar case)

$$\psi(r, z) = Rx^{(n+1)/4}(1-x)^{1/2}\mathcal{G}(x, y). \tag{6.2}$$

These transform (2.4) into

$$\mathcal{G}_{yyy} - n(1-x)\mathcal{G}_y^2 + \tfrac{1}{2}[n+1-(n+3)x]\mathcal{G}\mathcal{G}_{yy} = -\tfrac{1}{2}y\{1-x+p[(3-n)x+n-1]\}x^{(1-n)/2}\mathcal{G}_{yy}$$

$$+(p-pn-1)x^{(1-n)/2}(1-x)\mathcal{G}_y + 2x(1-x)[\mathcal{G}_y\mathcal{G}_{xy} - \mathcal{G}_x\mathcal{G}_{yy}] - 2px^{(3-n)/2}(1-x)\mathcal{G}_{xy} \tag{6.3}$$

with the boundary conditions

$$\mathcal{G} = 0, \quad \mathcal{G}_y = p \quad \text{on} \quad y = 0 \quad \text{and} \quad \mathcal{G}_y \sim 0 \quad \text{as} \quad y \to \infty \quad \text{over} \quad 0 \leqslant x \leqslant 1. \tag{6.4}$$

It readily transpires that (6.3) does recover (4.2) when $x = 0$ and, with a minor transformation, (5.4) at $x = 1$ as planned; furthermore, on setting $n = 1$, (6.3) recovers a corresponding form given by Jensen (1995). The axisymmetric version of (6.3) follows by similar means but with $x^{(n+1)/4}$ in (6.2) replaced by $x^{(n+3)/4}$.

Of course (6.3) is also singular parabolic for $0 \leqslant n \leqslant 1$ and so whether it be SP0, SP1 or the m sub type of either, we choose to solve it in a manner akin to boundary value problems described by elliptic differential equations. Further since gradients are $O(1)$ or less in (6.3), finite difference techniques, specifically second-order-accurate central differences, provide an appropriate approximation. Wang (1983, 1985) reports success in solving finite difference representations of singular parabolic equations using the method of successive over-relaxation, so in view of its simplicity that was the first technique employed. Unfortunately our fortune was at best mixed: convergence/numerical-stability was achieved only with severe under-relaxation, and even then only after various fixes reminiscent of those employed by Dennis (1972). Moreover we obtained convergence for only some (n, p) and even then only after several hundred thousand iterations! Foda & Cox (1980) on the other hand chose a successive-approximation implicit scheme to solve a second-order-accurate finite difference representation of (2.4) over a domain removed from $r = 0$ and R, the ends being patched to appropriate asymptotic solutions. This technique proved ideal for our purposes although of course patching was not required with (6.3).

Here a solution to the whole field is obtained simultaneously. The procedure begins by formally writing $\mathcal{G} = \mathcal{G}_0 + \mathcal{G}_1$, with the assumption that $\mathcal{G}_0$ is known and $\mathcal{G}_1/\mathcal{G}_0 \ll 1$. Substitution into (6.3) and neglect of quadratic terms in $\mathcal{G}_1$ leads to a linearized version of (6.3) which is then discretized with second-order-accurate central differences. Difference equations at each node in the finite difference mesh of $N = I \times J$ unknowns give rise to a set of simultaneous linear equations which may be written as a matrix equation $\boldsymbol{AX} = \boldsymbol{B}$. Coefficients in the $N \times N$-dimensional matrix $\boldsymbol{A}$ and N-dimensional matrix $\boldsymbol{B}$, are given in terms of $\mathcal{G}_0$, while the N-dimensional

matrix $\boldsymbol{X}$ contains the unknown $\mathscr{G}_1$. But because $\boldsymbol{A}$ is square, non-symmetric, sparse and non-banded, conventional elimination methods for solving the linear system are inappropriate, as is Cholesky decomposition. The method of conjugate gradients (which is essentially a relaxation method) on the other hand is apt, although before proceeding the problem must be reset such that the coefficient matrix is symmetric and positive definite. Then, if $\mathscr{G}_0^k$ is the kth approximation to the difference equation at a particular node, the $(k+1)$th approximation at that node is given by $\mathscr{G}^{k+1} = \mathscr{G}_0^k + \mathscr{G}_1$, where $\mathscr{G}_1 \to 0$ as $k \to \infty$.

We employed a square mesh with I unknowns in the x-direction and J unknowns in y. J typically exceeded I by a factor of at least four depending upon n and p, and was chosen to ensure the boundary condition $G_y \sim 0$ was well satisfied at both $x = 0$ and 1 for large y. Tests revealed little if any dependence on mesh size for $I \geqslant 5$, but because spanwise detail suffered at the lower bound we typically set $I = 10$. Iteration continued until the largest $|\mathscr{G}_1/\mathscr{G}_0^k|$ in the mesh fell below 1×10^{-6}. Appropriate control of x in (6.3) permitted calculation of (4.5) or (4.7) or (5.4) throughout the domain and these were used as test cases. In each case four iterations from any initial values for $\mathscr{G}_0$ were enough to satisfy our convergence criteria and yield results in agreement (to within five significant figures) with Runge–Kutta calculations. To check variations in x we calculated the SP0m case $n = 1$, $p = \frac{1}{2}$, which Jensen (1995) has solved by marching techniques; our results closely concur. This check took about 100 iterations, although some SP1 and SP1m cases took nearly ten times that. Computations were done on Decstation 5000/200's using double-precision arithmetic. When optimally compiled the time scale for calculation to our prescribed level of convergence varied, depending upon the value of N, from a few minutes to several days.

7. Results and discussion

We should like the governing boundary layer equation to exhibit each of the singular parabolic types 0, 0m and 1, 1m, and this can be achieved (see §3) with the parameter range $n \in [0, 1]$, $p \in (0, 2]$. A wide selection of cases was solved in this range, although only those considered representative are presented here. Accordingly, we present solutions only to the planar equation (6.3) and, when discussing $n = 1$, restrict attention to stagnation points defined by the upper branch of figure 1 (see §4), as these give rise to forward-only flow.

7.1. *Diffusivity and singular parabolic behaviour*

Contours of diffusivity for three types of flow are shown in figures 4, 5 and 6. We begin with type-0m. Here vorticity is convected only in the negative r-direction but the diffusivity is of mixed sign. Such situations occur for $n = 1$, $0 < p < 1$. Two cases are sketched in figure 4: that for p just less than unity and that for p just greater than its value at which $\chi''(0)$ is first negative (see figures 1, 2(*a*)), i.e. at which v_r is first a maximum at the surface. Corresponding velocity profiles are given in figure 7. As expected from our discussions in §§3,4 the diffusivity is negative for $0 \leqslant x < 1$ on $y = 0$, and, as can occur for unsteady separated stagnation points, for some $y \geqslant 0$ on $x = 0$. The extent of the region in x, y space where the diffusivity is negative, however, is seen to decrease as p increases toward unity, at which point it vanishes; (2.4) is then SP0 (figure 6*a*).

Vorticity is convected in both the positive and negative r-direction, and diffusivity is mixed, in type-1m flows for which $0 \leqslant n < 1$, $0 < p < 1$. But steady stagnation points, which arise in such flows (see §4), do not admit solutions with negative diffusivity.

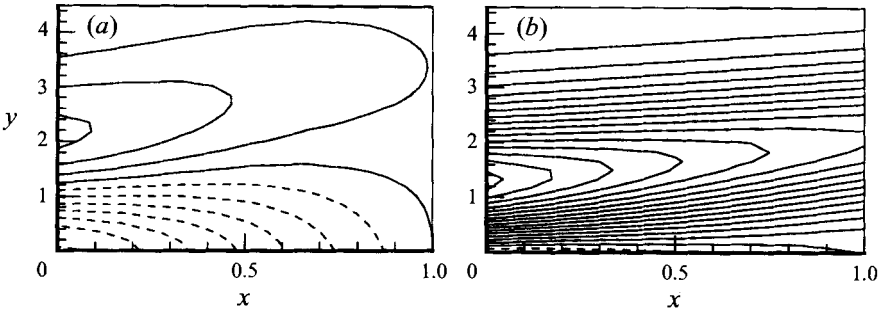

FIGURE 4. Contours of diffusivity in x, y space for SP0m flows: (*a*) $n = 1$, $p = 0.36$; (*b*) $n = 1$, $p = 0.95$. Full lines, positive diffusivity; dashed lines, negative diffusivity. For corresponding velocity profiles see figure 7.

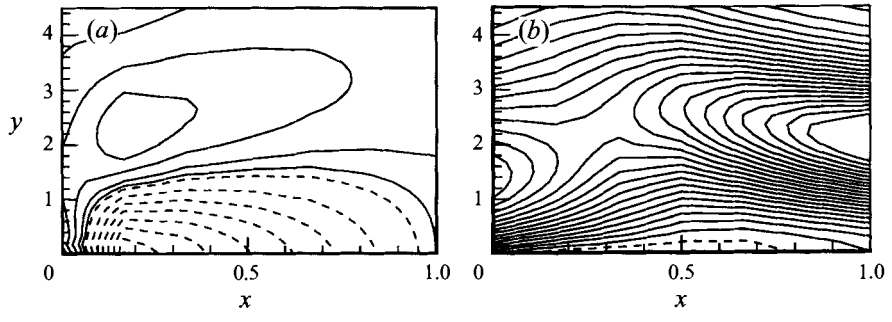

FIGURE 5. As figure 4 but: for SP1m flows; (*a*) $n = 0.95$, $p = 0.36$; (*b*) $n = 0$, $p = 0.95$. For corresponding velocity profiles see figure 8.

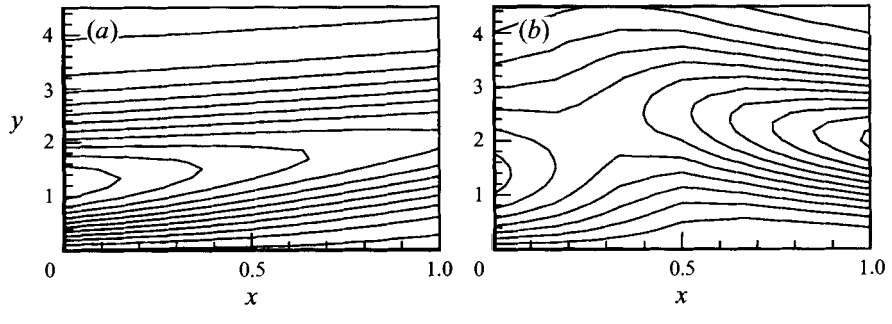

FIGURE 6. Contours of diffusivity in x, y space for: (*a*) SP0 flow $n = 1$, $p = 1$; (*b*) SP1 flow $n = 0$, $p = 1$. For corresponding velocity profiles see figure 9.

The velocity field at the origin is therefore quite different to its counterpart in the previous case, as we see by comparing figures 7(*a*) and 8(*a*). Moreover the region of negative diffusivity in such flows is limited to some y (including zero) in $0 < x < 1$, as is evident in figure 5 and acts, a short distance from the origin, to lower the velocity gradient at the surface (figure 8*a*). Again, the extent of the region of negative diffusivity is seen to diminish as p approaches unity, where it vanishes; (2.4) is then SP1 (figure 6*b*).

Contours of diffusivity for SP1 and SP0 are a straightforward progression from their predecessors with mixed diffusivity (compare figures 4*b* and 5*b* with figure 6).

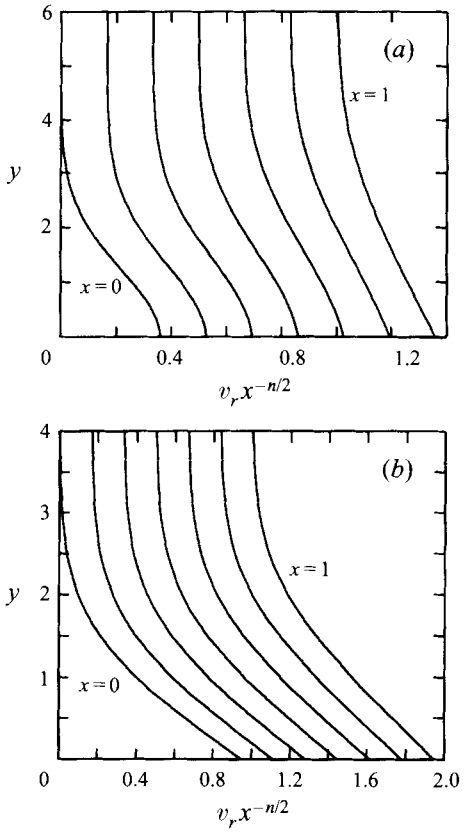

FIGURE 7. Profiles of radial velocity for $n = 1$: (*a*) $p = 0.36$, (*b*) $p = 0.95$; the profiles are equispaced throughout $x \in [0, 1]$.

But the contours for SP0 are markedly different from those for SP1. Specifically while for the most part diffusivity decreases with increasing x for SP0, there is a saddle at some x removed from 0 or 1 for SP1 and gives rise to a velocity field which penetrates to larger y; see figure 9.

Few if any of these features are evident from contours of the stream function ψ, although overlaying the displacement thickness $\delta^* = x^{(1-n)/4}(1-x)^{1/2}G(x,\infty)/p$ as we have done in figure 10 is helpful. Figures 10 and 11 also reflect the fact that δ^* is zero at $x = 0$ for steady separated stagnation points and non-zero at $x = 0$ for unsteady separated stagnation points (see §4). We further note (figure 11) that the maximum value of δ^* increases as p diminishes (see also §7.3); this is in accord with the role of p, which acts to accelerate material points in the flow for $p > 1$ and decelerate them for $p < 1$. Furthermore, while δ^* is clearly a maximum at $r = 0$ for SP0 and SP0m flows, the maximum location for SP1 and SP1m flows varies with p, from near $r/R = 0.5$ for $p \gg 1$, to closer to the leading edge as p diminishes. Figure 11 also suggests that the peak values of δ^* do not vary much with n for given p, and results for other $0 < n < 1$ (not shown) concur. Of course the detailed variation of δ^* with r as $r \to 0$ does vary with n, as is to be expected from the appropriate asymptotic form of δ^*.

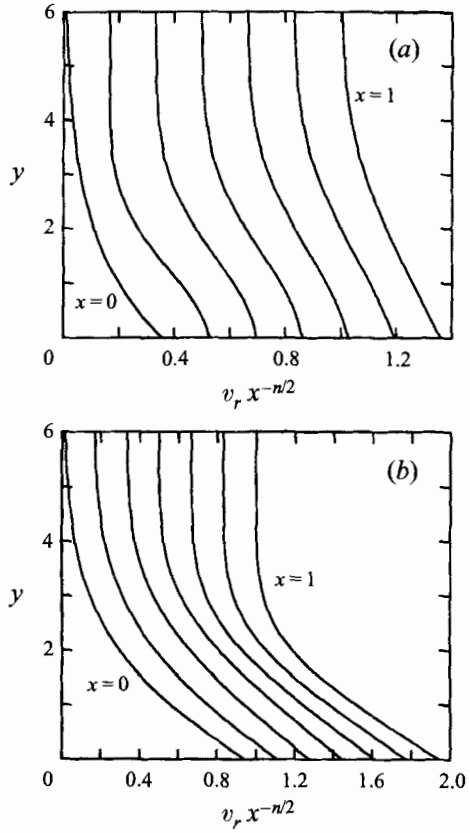

FIGURE 8. Profiles of radial velocity for (*a*) $n = 0.95$, $p = 0.36$ and (*b*) $n = 0$ with $p = 0.95$; the profiles are equispaced throughout $x \in [0, 1]$.

7.2. *Surface shear stress and drag*

Of particular interest are the drag on the surface and the distribution of shear stress along it. Let C_f be the local skin friction coefficient defined by the shear stress on the surface divided by $\rho \bar{v}_R^{*2}$, where $\bar{v}_R^*$ is the surface velocity at $\bar{r} = \bar{R}$ and ρ the density, and introduce a Reynolds number as $Re = \bar{v}_R^* \bar{R}/\nu$. Then for $C_f \geqslant 0$ we have $C_f Re^{1/2} = -x^{(3n-1)/4}(1-x)^{1/2}\mathscr{G}_{yy}(x,0)$, although for presentation purposes it is appropriate to write

$$p^{-3/2}\tau = p^{-3/2}\left(\frac{R-r}{R}\right)^{1/2}\left(\frac{r}{R}\right)^{(1-3n)/2} C_f Re^{1/2} = -p^{-3/2}\left(\frac{R}{R+r}\right)^{1/2}\mathscr{G}_{yy}(r,0) \quad (7.1)$$

so that

$$p^{-3/2}\tau \sim -p^{-3/2}\mathscr{G}_{yy}(0,0) = -\lambda''(0) \quad \text{or} \quad -p^{-3/2}\chi''(0)|_{\text{Upper branch}} \quad \text{as} \quad r \to 0,$$

while

$$p^{-3/2}\tau \sim -p^{-3/2}\frac{1}{\sqrt{2}}\mathscr{G}_{yy}(1,0) = g''(0) \quad \text{as} \quad r \to R.$$

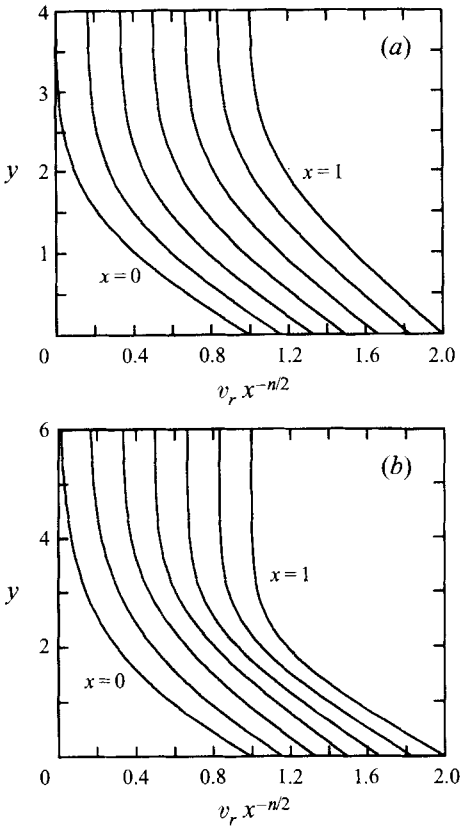

FIGURE 9. Profiles of radial velocity for (*a*) $n = 1$, $p = 1$ and (*b*) $n = 0$, $p = 1$; the profiles are equispaced throughout $x \in [0, 1]$.

Correspondingly we define the drag coefficient C_D as the drag per unit width on two sides of the surface divided by $\rho \bar{v}_R^{*2}$; then for $C_D \geqslant 0$ we have

$$C_D Re^{1/2} = -\int_0^1 x^{(3n-3)/4}(1-x)^{-1/2}\mathscr{G}_{yy}(x,0)\mathrm{d}x. \tag{7.2}$$

Consider first a surface of finite length moving in its own plane at constant velocity from its source at $x = 0$. Then $n = 0$, $p = 1$ and the flow field is asymptotic to a Blasius (1908) boundary layer at the leading edge and a Sakiadis (1961) layer at the origin. The ensuing distributions of τ are sketched in figure 12 along with τ for Stewartson's (1951) impulsively started semi-infinite flat plate (that achieves constant velocity in its own plane). Observe that beyond a mutual recovery of Blasius's result at $r/R = 1$ the two distributions of τ share little in common: Stewartson's curve (first obtained by Hall 1969 and Dennis 1972) monotonically increases from the leading edge while the present curve first decreases before increasing. Of course the flow field at $r = 0$ is vastly different in each problem: in our case the surface is continually produced at $r = 0$ giving rise to a steady stagnation point flow (see §4), while at the same location Stewartson's boundary layer is asymptotic to a Rayleigh (1911) shear layer (i.e. the flow generated by starting an infinite flat plate to move in its own plane at constant velocity). Here there is no stagnation point but rather an essential singularity (a Stewartson singularity) which is manifested as a solution that is not

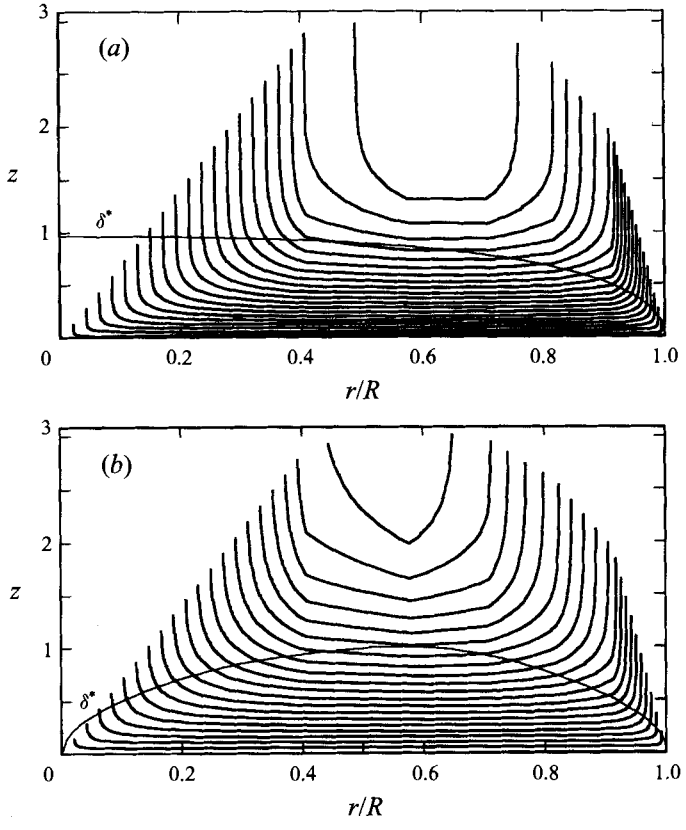

FIGURE 10. Distribution of the similarity variable ψ for (*a*) $n = 1$, $p = 1$ and (*b*) $n = 0$, $p = 1$ with concurrent variations of δ^*.

analytically continuous to $x < 0$, even though all derivatives with respect to $(1-x)^{-1}$ (an appropriate independent variable which arises from the similarity transformation) are continuous at $x = 0$. Physically, the region $r/R \in [0, 1]$ is that in which the boundary layer at the leading edge is aware of and interacts with its counterpart from the origin. Thus, because the two curves for τ are so different, it is evident that events at the origin are not local but profoundly affect the whole flow field.

Turning then to the drag, we note that the while $C_D Re^{1/2} = 1.3282$ and 1.7759 for Blasius and Sakiadis boundary layers respectively, the present layer ($n = 0$, $p = 1$) yields a value of $C_D Re^{1/2} = 2.2297$. This higher level is meaningful physically in view of the interacting leading edge and origin boundary layers but is not to be expected from figure 12 which, as is evident from (7.1) gives a somewhat deceptive view of shear stress.

Distributions of τ for other values of p for $n = 0$ and $n = 1$ are also drawn in figure 12. Since $\lambda''(0)$ depends on n but not p for $n < 1$, the same (with p) steady stagnation point flow applies at $r = 0$ in each SP1 or SP1m case. But that is not so for $n = 1$, where the flow now contains an unsteady stagnation point whose details vary with p, as we saw previously in figure 2(*a*). Interestingly, SP0 or SP0m flows cause less drag at given p than their SP1 or SP1m counterparts, as we see in figure 13. The reason, as is evident from figures 4(*a*) and 5(*a*), 4(*b*) and 5(*b*), and 6(*a*) and 6(*b*), is because of differences in the diffusion field resulting from different types of stagnation points at $r = 0$. But it would be wrong to gain the impression that all SP1

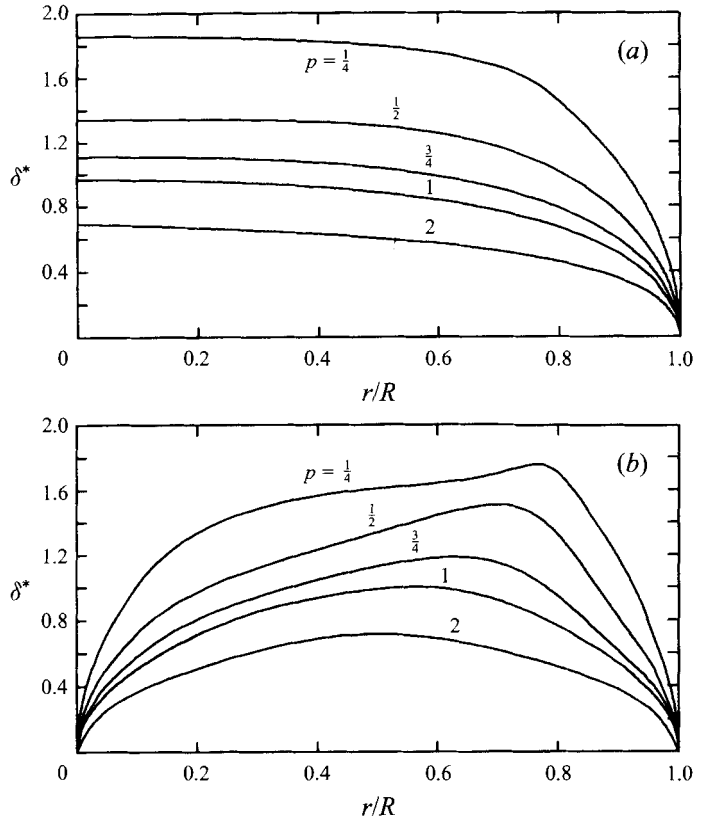

FIGURE 11. The variation of δ^* with r/R for (*a*) $n = 1$ and (*b*) $n = 0$ for various values of p.

and SP1m flows lead to drag higher than what would arise in Blasius or Sakiadis flow: indeed, as we see from figure 13, the drag is lower than these reference points for many extensible ($0 < n < 1$) and some non-extensible ($n = 0$) surface flows.

7.3. *A note on the case* $0 < p \ll 1$

Physical arguments suggest that the more rapidly (slowly) the surface grows, the greater (lower) the drag, and this is reflected in figure 13. But as noted in §4 there is a value of p, p_{crit} say, below which there is a change in the direction of surface shear stress (see figure 2*a*) and it is appropriate to ask whether solutions to (6.3) and (6.4) exist for $p < p_{crit}$? Local stress reversals correspond of course to a decrease in drag, but they also indicate v_r is a maximum not at the surface but within the boundary layer proper. The dilemma unfortunately is that in the absence of imposed pressure gradients and with a flow driven by an extensible surface such as we have, it is difficult to imagine local stress reversals occurring. Of course nature prudently avoids the dilemma by setting $p = \frac{3}{8}$ for gravity-viscous ($n = 1$) planar spreading of an oil slick of constant mass (see Buckmaster 1973) and $p = \frac{1}{4}$ for its axisymmetric counterpart, each a tad higher than their respective p_{crit} values of approximately 0.3551 and 0.2378. But nature notwithstanding, we were able to obtain numerical solutions for $p < p_{crit}$ which satisfied our convergence criteria (see §6); two such results are sketched in figures 11 and 12. So we then asked whether there is a positive value of p at which $C_D Re^{1/2} = 0$, and if so, do solutions exist at smaller values of p?

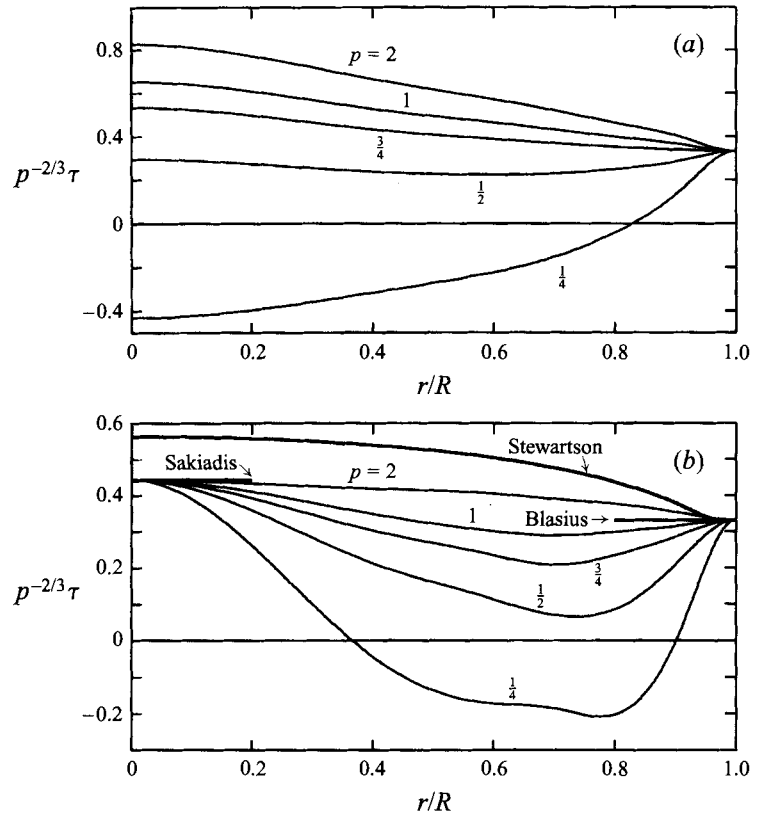

FIGURE 12. Variation with r/R of the shear-stress-related variable τ for (*a*) $n = 1$ and (*b*) $n = 0$ for various values of p.

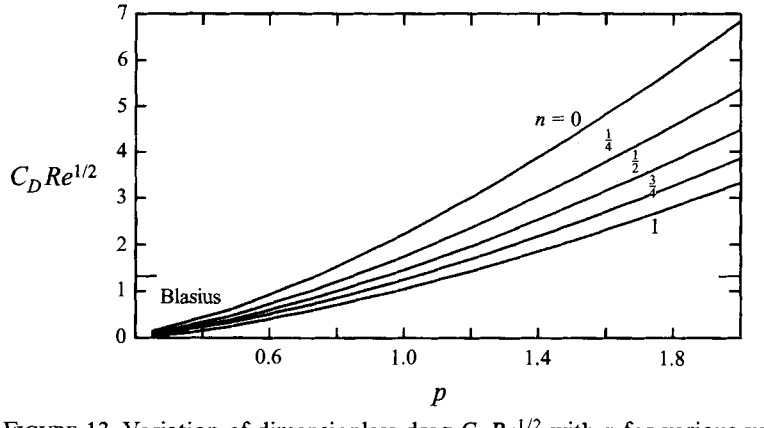

FIGURE 13. Variation of dimensionless drag $C_D Re^{1/2}$ with p for various values of n.

For SP1m flows the answers appear to be no and thus no; in that so far as we could ascertain numerically, $\lim_{p\to 0+} C_D Re^{1/2} > 0$. But for SP0m ($n = 1$) flows, the answers are yes and yes; indeed the lowest curve on figure 13 continues through zero (at $p \approx \frac{1}{2}p_{crit}$) to depict negative drag! Of course δ^* increases significantly as p decreases, so this drag result probably indicates breakdown of the long-wave assumption upon

which our analysis is based (which assumes the surface length $\bar{R}$ greatly exceeds the characteristic thickness of the boundary layer flow). But it is doubtful that the long-wave assumption has broken down at $p = p_{crit}$ and it would be most interesting to construct an experiment (at least for $n = 0$ spreading) to see just what does happen for $p < p_{crit}$.

8. Conclusions

A family of similarity solutions is shown to describe a class of unsteady boundary layers that form on flat extensible surfaces of finite but increasing length in otherwise stagnant surroundings. In this class the surface length $\bar{R}$ is assumed to grow with time as t^p where $p > 0$ and the velocity at any location $0 \leqslant \bar{r} \leqslant \bar{R}$ on the surface as $t^{p-np-1}\bar{r}^n$, where $n \geqslant 0$. It is further shown that although the equation comprising the similarity solution is parabolic, various combinations of n and p invoke regions of mixed mathematical diffusivity and reversals in the direction of convection of vorticity, rendering the equation singular parabolic. Such behaviour is herein classified according to whether the mathematical diffusivity is positive or mixed and whether or not there are reversals in the direction of convection of vorticity. It is further shown that such peculiarities affect the type of stagnation point, be it steady or unsteady separated, that is formed at the origin. Such details are important because conventional marching techniques to solve parabolic equations are shown to fail for all cases for which a steady stagnation point occurs at the origin; these cases must be treated in a manner akin to elliptic boundary value problems. The numerical solution of a wide range of cases in the parameter range $n \in [0, 1]$, $p \in (0, 2]$ reveal, amongst other things, that at specified p, extensible surfaces have lower drag than their non-extensible counterparts.

This work was supported by National Science Foundation grant OCE-9503456.

REFERENCES

BAN, S. D. & KUERTI, G. 1969 The interaction region in the boundary layer of a shock tube. *J. Fluid Mech.* **38**, 109–125.

BANKS, W. H. H. & ZATURSKA, M. B. 1986 Eigensolutions in boundary layer flow adjacent to a stretching wall. *IMA J. Appl. Maths* **36**, 263–273.

BLASIUS, H. 1908 Grenzschichten in Flüssigkeiten mit kleiner Reibund. *Z. Math. Phys.* **56**, 1–37.

BROWN, S. N. & STEWARTSON. K. 1965 On similarity solutions in the boundary layer equations with algebraic decay. *J. Fluid Mech.* **23**, 673–687.

BROWN, S. N. & STEWARTSON. K. 1969 Laminar separation. *Ann. Rev. Fluid Mech.* **1**, 45–72.

BUCKMASTER, J. 1973 Viscous-gravity spreading of an oil slick. *J. Fluid Mech.* **59**, 481–491.

CRANE, L. J. 1970 Flow past a stretching plate. *Z. Angew. Math. Phys.* **21**, 645–647.

DENNIS S. C. R. 1972 The motion of a viscous fluid past an impulsively started semi-infinite flat plate. *J. Inst. Maths. Applics.* **10**, 105–117.

FAY, J. A. 1969 The spread of oil slicks on a calm sea. In *Oil on the Sea* (ed D. P. Hoult), pp. 53–63. Plenum.

FODA, M. & COX, R. G. 1980 The spreading of thin liquid films on a water-air interface *J. Fluid Mech.* **101**, 33–51.

HALL, M. G. 1969 Boundary layer over an impulsively started flat plate. *Proc. Roy. Soc. Lond.* A **310**, 401–414.

JENSEN, O. E. 1995 The spreading of insoluble surfactant at the free surface of a deep fluid layer. *J. Fluid Mech.* **293**, 349–378.

LAM, S. H. & CROCCO, L. 1959 Note on the shock-induced unsteady laminar boundary layer on a semi-infinite flat plate. *J. Aero Sci.* **26**, 54–55.

MA, P. K. H. & HUI, W. H. 1990 Similarity solutions of the two-dimensional unsteady boundary-layer equations *J. Fluid Mech.* **216**, 537–559.

RAYLEIGH, LORD 1911 On the motion of solid bodies through viscous fluid. *Phil. Mag.* **21**, 697–711.

SAKIADIS, B. C. 1961 Boundary layer behavior on a continuous solid surface. *AIChEJ* **7**, 221–225.

STEWARTSON, K. 1951 On the impulsive motion of a flat plate in a viscous fluid. *Q. J. Mech. Appl. Maths* **4**, 182–198.

STUART, J. T. 1966 Double boundary layers in oscillatory viscous flow. *J. Fluid Mech.* **24**, 673–687.

TAYLOR, G. I. 1959 The dynamics of thin sheets of fluid. *Proc. Roy. Soc. Lond.* A **253** 289–295.

WALKER J. D. A. & DENNIS S. C. R. 1972 The boundary layer in a shock tube. *J. Fluid Mech.* **56**, 19–47.

WANG, C. Y. 1984 The three dimensional flow due to a stretching flat surface. *Phys. Fluids* **27**, 1915–1917.

WANG, J. C. T. 1983 On the numerical methods for the singular parabolic equations in fluid dynamics. *J. Comput. Phys.* **52**, 464–479.

WANG, J. C. T. 1985 Renewed studies on the unsteady boundary layers governed by singular parabolic equations. *J. Fluid Mech.* **155**, 431–427.